Extended Experiments for Takeoff and Landing on Slopes via Inclined Hovering with a Tethered Aerial Robot. Technical Attachment to: M. Tognon, A. Testa, E. Rossi and A. Franchi " Takeoff and Landing on Slopes via Inclined Hovering with a Tethered Aerial Robot " published in the 2016 IEEE/RSJ International Conference on Intelligent Robots and Systems Daejeon, South Korea, Oct. 2016

Marco Tognon, Andrea Testa, Enrica Rossi, Antonio Franchi

Extended Experiments for Takeoff and Landing on Slopes via Inclined Hovering with a Tethered Aerial Robot

Technical Attachment to:
M. Tognon, A. Testa, E. Rossi and A. Franchi
"Takeoff and Landing on Slopes via Inclined Hovering with a Tethered Aerial Robot"
published in the *2016 IEEE/RSJ International Conference on Intelligent Robots and Systems*
Daejeon, South Korea, Oct. 2016

Marco Tognon[1], Andrea Testa[2], Enrica Rossi[1] and Antonio Franchi[1]

I. Introduction

This document is a technical attachment to [1], a paper which provides a study and a methodology for landing and takeoff using a passive tether attached to the aerial platform. This document includes a proof of the flatness of the output $\mathbf{y}^{f_L}$ (in Section II) and extended results of the experiments not included in [1] because of page limits (in Section III).

The reader interested in the analysis and control of tethered aerial vehicles is also referred to [2], [3], where flatness, controllability and observability is studied, to [4] where the case of a moving base is thoroughly analyzed, and to [5], [6] where the case of multiple tethered vehicles is investigated.

A. Aerial physical interaction

Tethered aerial vehicles constitute an example of aerial vehicles physically interacting with the external environment. For the reader interested in this rapidly expanding and broad topic we also suggest the reading of [7], where a force nonlinear observer for aerial vehicles is proposed, of [8], where an IDA-PBC controller is used for modulating the physical interaction of aerial robots, of [9], [10] where fully actuated platforms for full wrench exertion are presented, of [11]–[13] where the capabilities of exerting forces with a tool are studied, and finally of [14]–[16] where aerial manipulators with elastic-joint arms are modeled and their controllability properties discovered.

II. Differential flatness with respect to $\mathbf{y}^{f_L}$

Let us consider the output $\mathbf{y}^{f_L} = [y_1^{f_L}\ y_2^{f_L}\ y_3^{f_L}\ y_4^{f_L}]^T = [\varphi\ \delta\ f_L\ \psi_R]^T \in \mathbb{R}^4$. In this section we shall demonstrate that the tethered system in [1] is differential flat with respect to $\mathbf{y}^{f_L}$. For this purpose the state and the inputs have to be written as an algebraic function of the output and its derivatives.

We get directly that $\mathbf{q} = [y_1^{f_L}\ y_2^{f_L}]^T$ and $\dot{\mathbf{q}} = [\dot{y}_1^{f_L}\ \dot{y}_2^{f_L}]^T$. Then from (4) in the paper, we can write f_R and $\mathbf{z}_R$ as an algebraic function of $\mathbf{y}^{f_L}$ and its derivatives as:

$$f_R = \left\|\mathbf{f}_R(\mathbf{y}^{f_L}, \dot{\mathbf{y}}^{f_L}, \ddot{\mathbf{y}}^{f_L})\right\|, \quad \mathbf{z}_R = \frac{\mathbf{f}_R(\mathbf{y}^{f_L}, \dot{\mathbf{y}}^{f_L}, \ddot{\mathbf{y}}^{f_L})}{\left\|\mathbf{f}_R(\mathbf{y}^{f_L}, \dot{\mathbf{y}}^{f_L}, \ddot{\mathbf{y}}^{f_L})\right\|}, \quad \text{(TR.1)}$$

where $\mathbf{f}_R = -m_R\ddot{\mathbf{p}}_R(\mathbf{y}^{f_L}, \dot{\mathbf{y}}^{f_L}, \ddot{\mathbf{y}}^{f_L}) - m_R g\mathbf{z}_W - y_3^{f_L}\mathbf{d}(\mathbf{y}^{f_L})$. Equation (TR.1), together with $y_4^{f_L}$, let us define the attitude of the vehicle as a function of $\mathbf{y}^{f_L}$ and its derivatives. In fact, given $y_4^{f_L}$ we can define $\mathbf{x}'_R = \mathbf{R}_\mathbf{z}(y_4^{f_L})\mathbf{e}_1$, where $\mathbf{R}_\mathbf{z}(y_4^{f_L})$ is the rotation matrix describing the rotation of $y_4^{f_L}$ along $\mathbf{z}_W$. The attitude is computed creating an orthonormal basis out of $\mathbf{x}'_R$ and $\mathbf{z}_R$, given by $\mathbf{R}_R(\mathbf{y}^{f_L}, \dot{\mathbf{y}}^{f_L}, \ddot{\mathbf{y}}^{f_L}) = [\mathbf{x}_R\ \mathbf{y}_R\ \mathbf{z}_R]$ where,

$$\mathbf{y}_R = \frac{\mathbf{z}_R \times \mathbf{x}'_R}{\|\mathbf{z}_R \times \mathbf{x}'_R\|}, \qquad \mathbf{x}_R = \frac{\mathbf{y}_R \times \mathbf{z}_R}{\|\mathbf{y}_R \times \mathbf{z}_R\|}.$$

Differentiating $\mathbf{R}_R(\mathbf{y}^{f_L}, \dot{\mathbf{y}}^{f_L}, \ddot{\mathbf{y}}^{f_L})$ and using (2) of [1], we can write $\boldsymbol{\omega}_R$ and $\boldsymbol{\tau}_R$ as a function of $\mathbf{y}^{f_L}$ and its derivatives. Finally, we were able to write state and inputs as a function of $\mathbf{y}^{f_L}$ and its derivatives, thus proving the differential flatness of the system with respect to $\mathbf{y}^{f_L}$.

III. Experimental Validation

In this section we show the main results of an experimental campaign aimed at validating the efficacy of our method for the problem of landing (and takeoff) an aerial vehicle on a sloped surface.

The vehicle for our experiments is a Mikrokopter quadrotor weighting about 1[Kg] and having a maximum thrust for each propeller of 6[N]. We built a simple sloped surface based on a structure made of steel bars fixed to the ground by heavy loads. The vehicle is equipped with a light cable ending with a triple hook at its extremity. The other end of the link is attached to the vehicle as close as possible to its center of mass. The link has a length of 1[m] and a mass of less than 0.01[Kg], thus negligible w.r.t. the vehicle one.

To hook the free extremity of the link to the structure, we placed an horizontal slack cable passing through the anchor point $\mathbf{p}_A$ (a priori decided). A simple maneuver lets the vehicle hook the horizontal cable resulting tethered to the anchor point, as it is shown in Fig. 6.

[1]LAAS-CNRS, Université de Toulouse, CNRS, Toulouse, France, mtognon@laas.fr, erossi@laas.fr, antonio.franchi@laas.fr
[2]Department of Engineering, Università del Salento, via per Monteroni, 73100 Lecce, Italy andrea.testa@unisalento.it

Partially funded by the European Union's Horizon 2020 research and innovation programme under grant agreement No 644271 AEROARMS.

The controller, fully implemented in *Matlab-Simulink*, sends the desired rotational speed of each propeller at a frequency of 500[Hz]. The communications with the robot and the PC are done through a physical serial cable.

In order to retrieve the state of the system we use a motion capture system to measure the position and the yaw angle of the vehicle with a frequency of 120[Hz]. The linear velocity is computed by the numerical derivation of the measured position. Notice that, when the link is taut, the motion capture system emulates two encoders that measure φ and δ, and a magnetometer for the Yaw. Finally we used an on-board IMU (accelerometer and gyroscope) to complete the measurement of the attitude estimating the remaining Euler angles, Roll and Pitch, and the angular rate, $\boldsymbol{\omega}_R$.

A. Sinusoidal trajectories

In order to validate and test the performances of the proposed hierarchical controller we tried to track some highly dynamical trajectories showing the ability to independently track φ and ϑ_A, at the same time.

In particular we shall show the results of the control action for three different sinusoidal trajectories: 1) sinusoidal trajectory with time varying frequency on φ while keeping ϑ_A constant, 2) sinusoidal trajectory with time varying frequency on ϑ_A while keeping φ constant, and 3) sinusoidal trajectory with fixed frequency on both φ and ϑ_A.

The first two tests are done firstly to see that the proposed controller can track a desired trajectory on φ or ϑ_A, independently. Secondly we want to show which is the maximum feasible frequency for both dynamics.

In the first experiment we fixed the desired ϑ_A^d at $15[^\circ]$. In this way we assured a sufficiently high tension in order to limit nominal negative tension value during the experiment. The desired sinusoidal trajectory $\varphi^d(t)$ starts with a frequency equal to $\omega_\varphi = \frac{2\pi}{4}\left[\frac{\text{rad}}{\text{s}}\right]$ and it increases linearly until the value of about $\omega_\varphi = \frac{4\pi}{5}\left[\frac{\text{rad}}{\text{s}}\right]$ for which the system becomes unstable. From Fig. 1 one can see that the tracking of φ and ϑ_A degrades with the increasing of the frequency of the sinusoidal trajectory.

The second test is the dual, indeed we propose a sinusoidal desired trajectory with varying frequency on ϑ_A while keeping a desired constant $\varphi^d = 45[^\circ]$. For what concerns the frequency of the sinusoidal desired trajectory $\vartheta_A^d(t)$, it starts from a value of $\omega_{\vartheta_A} = \frac{2\pi}{6}\left[\frac{\text{rad}}{\text{s}}\right]$ and increase up to a value of about $\omega_{\vartheta_A} = \frac{8\pi}{9}\left[\frac{\text{rad}}{\text{s}}\right]$. After that, as it is possible to see from the plots in Fig. 2, the tracking error becomes very high. However, the system remains always stable.

Finally we gave as reference a sinusoidal trajectory on both φ and ϑ_A. The two signals have different frequency and phases, in particular $\omega_\varphi = \frac{2\pi}{4}\left[\frac{\text{rad}}{\text{s}}\right]$ and $\omega_{\vartheta_A} = \frac{2\pi}{6}\left[\frac{\text{rad}}{\text{s}}\right]$, respectively. The results can be seen in Fig. 3. As one can see the trajectories are both tracked with a sufficiently small error. This analysis finally shows that the proposed controller is able to independently track sufficiently slow time varying desired trajectories on both φ and ϑ_A, with small tracking errors. We did not report the results of the tracking of δ because they are analogous to the ones related to φ.

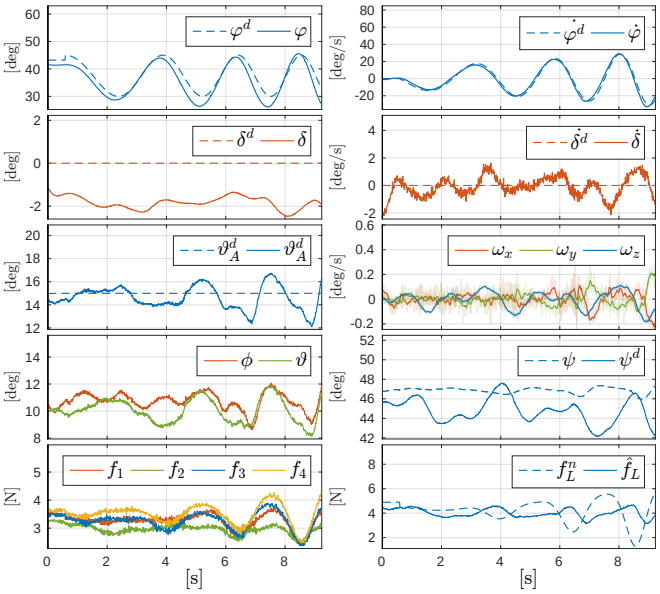

Fig. 1: Tracking of a sinusoidal input on elevation with varying period with fixed attitude

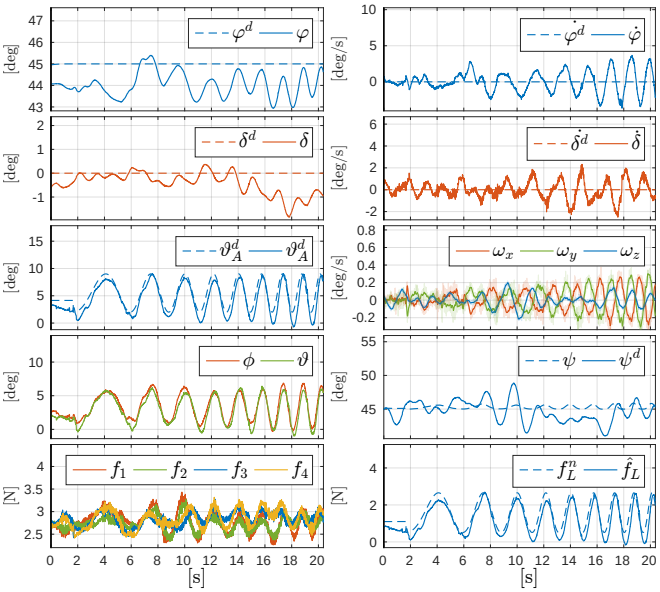

Fig. 2: Tracking of a desired sinusoidal trajectory of ϑ_A with varying frequency and fixed φ.

B. Landing with the free-flight approach

In this paragraph we describe the results obtained trying to land on a surface tilted by $30[^\circ]$ using the free-flight approach. In particular we want to show that using a classical position controller is not possible to land on such sloped surfaces. Indeed, as demonstrated in the paper, this is possible only using a maneuver based approach, for which the landing is achieved only carefully planning the trajectory and precisely tracking it.

The dynamic of the experiment is quite simple. The vehicle starts in free-flight condition and tries to land on a desired point of the surface following a simple descending trajectory along $\mathbf{z}_W$. Finally, the robot switches off the motors

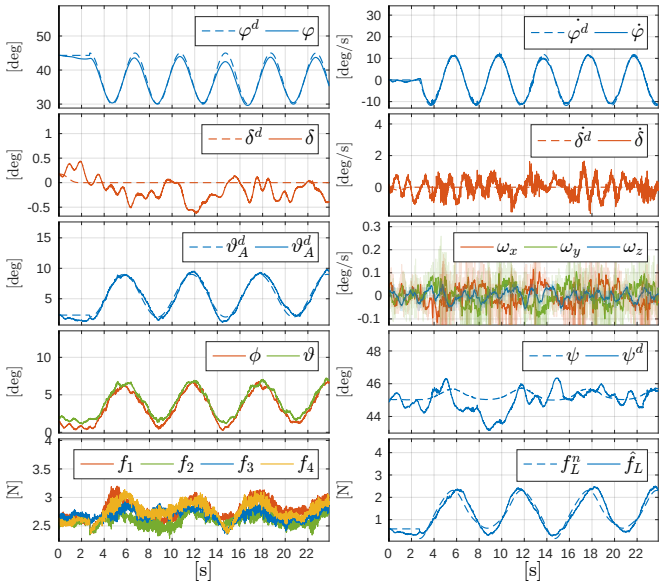

Fig. 3: Tracking of a desired sinusoidal trajectory on both φ and ϑ_A with fixed period.

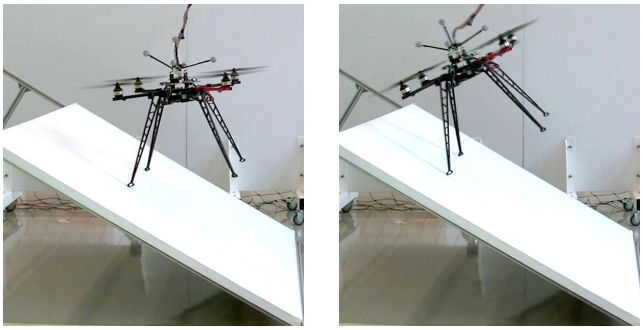

(a) Desired landing position on the surface.

(b) Desired landing position below the surface. The picture shows the vehicle the instant before crashing on the surface.

Fig. 4: Landing with the free-flight approach.

when the surface is reached.

Giving as desired position a point on the surface, the vehicle touches it with only two landers and remains in an almost hovering condition (see Fig. 4a). Then, when the motors are switched off the vehicle hits the surface with the others two landers and slides down along the surface.

In order to make the attitude parallel to the surface, one can try to move the desired landing point along the normal to the surface. Placing the desired landing point above the surface, the vehicle will fly in the desired position without even touching it. On the other hand, placing the desired landing position below the surface, we obtain a result opposite with respect to the desired one. In fact, trying to reach the desired position the vehicle tilts toward the surface (see Fig. 4b) instead of adjusting the attitude according to the plane. Moreover, at a certain moment of the experiment, the two landers in contact with the surface loose the grip and the vehicle crashes on it.

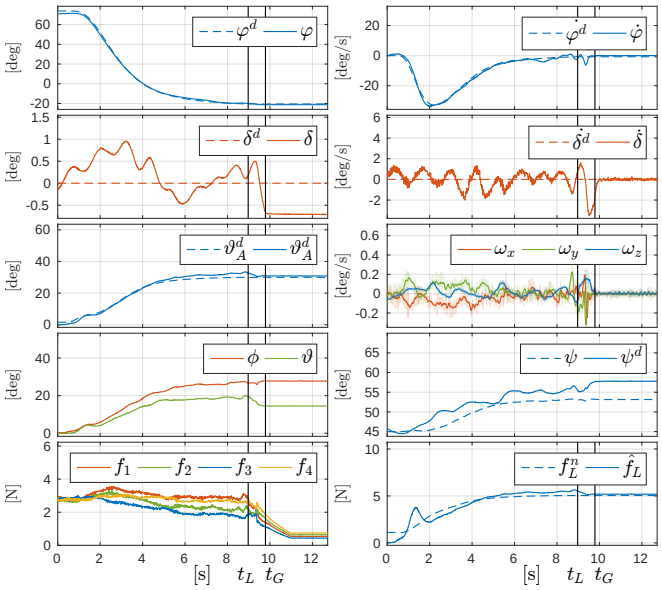

Fig. 5: Tracking of the desired landing maneuver. In the plot of $\boldsymbol{\omega}_R$, the solid and opaque lines correspond to the filtered and unfiltered data, respectively. f_L^n is the nominal stress given by the particular trajectory, whereas $\hat{f}_L$ is the estimated stress from the knowledge of the model, state and inputs.

In general we also noticed a high flight instability when close to the surface due to aerodynamic effects.

C. Landing with passive-tethered approach

The goal of the experiment is to automatically land the robot on a surface, tilted by 30[°]. The maneuver starts with the vehicle in a free-flight configuration and consists of five phases (see Fig. 6):

(a) approach to the anchor point making the hook in contact with the anchoring horizontal cable,

(b) hook the horizontal cable,

(c) stretch the link making it taut,

(d) track the desired trajectory $\mathbf{y}^{\vartheta_A d}(t)$,

(e) turn-off the propellers after the landing.

Although not necessary, the global maneuver is done moving on the plane $\mathscr{P}_M$, in order to simplify the phases (a-c). During phases (a-c) the vehicle is controlled by a standard position controller. In particular, to make the link taut, we simply give as reference a position that lies outside the sphere $\mathscr{S}_l(\mathbf{p}_A)$. In this way the vehicle pulls the link while trying to reach that unreachable position. As soon as, at time t_0, the link is taut (detectable using a threshold in the position error) the controller presented in Sec. V of [1] is activated and a simple trajectory $\mathbf{y}^{\vartheta_A d}(t)$ is used as reference. Given the parameters of the system, in order to achieve the landing conditions, from Sec. III of the paper it results that:

$$\varphi^\star = -21.3[^\circ], \quad \delta^\star = 0[^\circ], \quad \vartheta_A^\star = 30[^\circ].$$

During the maneuver, $\psi_R^\star$ is set such that the frame of the vehicle is turned by 45[°] with respect to the link. Since the link is not perfectly attached to O_R, the tension creates an extra torque on the body that is properly compensated in

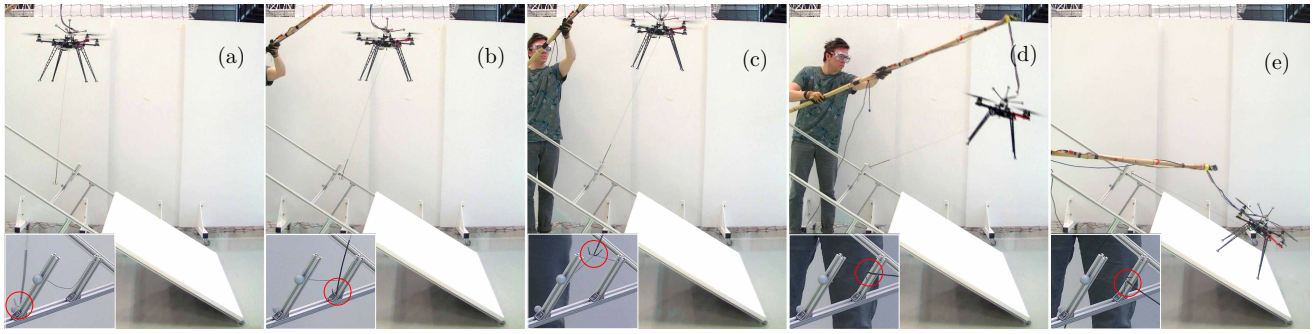

Fig. 6: Sequence of images of a real experiment. On the left bottom corner we show a zoom of the anchor point and the hook circled in red. The vehicle is attached by a cable to a pole from the top for security reasons and to connect the robot to the PC by a serial cable. Notice from Fig. (d) that this cable is always slack and does not perturbs the motion of the robot.

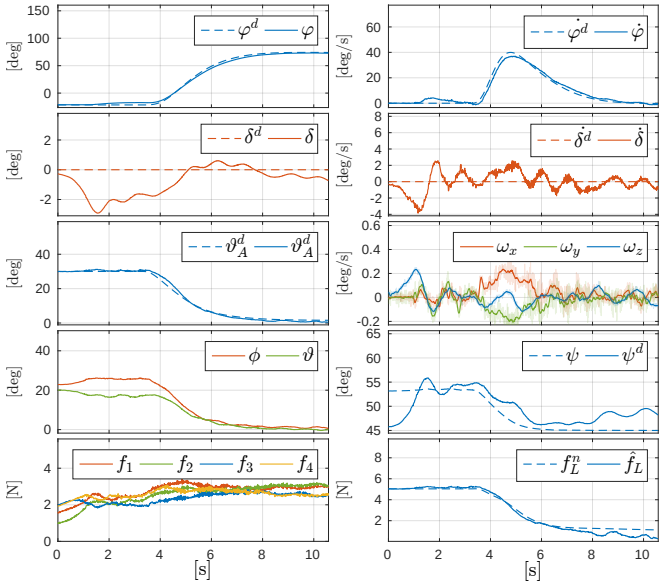

Fig. 7: Tracking of the desired takeoff maneuver from a slope with 30[°] of inclination using an optimal trajectory.

order to improve the tracking performances, a sensor based calibration [17] of these parameters is left as future study.

In Fig. 6 and 5 the results of the experiment are shown. At time t_L the surface is reached with a stable and safe maneuver thanks to the existence of inclined equilibria (see [1]) and the motors are turned off. Additionally, after t_G, one can see that the vehicle, thanks to the tether, does not slide on the surface.

D. Takeoff with passive-tethered approach

After the landing we also performed the dual maneuver: takeoff from a sloped surface. The robot starts from a plane with an inclination of 30[°] with motors off. First of all, we noticed that thanks to the tether the vehicle does not slide along the surface, differently from the case without the tether. After increasing the rotational speed on the propellers, the vehicle, using the proposed controller, follows a simple trajectory reaching a position far enough from the surface. At this point a standard position controller is activated and, following a simple position trajectory, the robot is able to detach the hook from the horizontal anchoring cable. In Fig. 7 we report the results of such experiment where one can see that the desired trajectory is well tracked. We report just the data relative to the maneuver while tethered, since the data from the trajectory tracking with the position controller are considered not very relevant.

In conclusion, using the proposed method it is possible to both takeoff and land from any surfaces with different inclinations. Furthermore, it is important to notice that it is possible to attach and detach the hook from the anchor completely autonomously passing from a free-flight to tethered condition and vice versa. This lets the method be easily applied for real tasks.

References

[1] M. Tognon, A. Testa, E. Rossi, and A. Franchi, "Takeoff and landing on slopes via inclined hovering with a tethered aerial robot," in *2016 IEEE/RSJ Int. Conf. on Intelligent Robots and Systems*, Daejeon, South Korea, Oct. 2016.

[2] M. Tognon and A. Franchi, "Nonlinear observer-based tracking control of link stress and elevation for a tethered aerial robot using inertial-only measurements," in *2015 IEEE Int. Conf. on Robotics and Automation*, Seattle, WA, May 2015, pp. 3994–3999.

[3] ——, "Dynamics, control, and estimation for aerial robots tethered by cables or bars," *CoRR*, vol. abs/1603.07567, 2016. [Online]. Available: http://arxiv.org/abs/1603.07567

[4] M. Tognon, S. S. Dash, and A. Franchi, "Observer-based control of position and tension for an aerial robot tethered to a moving platform," *IEEE Robotics and Automation Letters*, vol. 1, no. 2, pp. 732–737, 2016.

[5] M. Tognon and A. Franchi, "Control of motion and internal stresses for a chain of two underactuated aerial robots," in *14th European Control Conference*, Linz, Austria, Jul. 2015, pp. 1614–1619.

[6] ——, "Nonlinear observer for the control of bi-tethered multi aerial robots," in *2015 IEEE/RSJ Int. Conf. on Intelligent Robots and Systems*, Hamburg, Germany, Sep. 2015, pp. 1852–1857.

[7] B. Yüksel, C. Secchi, H. H. Bülthoff, and A. Franchi, "A nonlinear force observer for quadrotors and application to physical interactive tasks," in *2014 IEEE/ASME Int. Conf. on Advanced Intelligent Mechatronics*, Besançon, France, Jul. 2014, pp. 433–440.

[8] ——, "Reshaping the physical properties of a quadrotor through IDA-PBC and its application to aerial physical interaction," in *2014 IEEE Int. Conf. on Robotics and Automation*, Hong Kong, China, May. 2014, pp. 6258–6265.

[9] S. Rajappa, M. Ryll, H. H. Bülthoff, and A. Franchi, "Modeling, control and design optimization for a fully-actuated hexarotor aerial vehicle with tilted propellers," in *2015 IEEE Int. Conf. on Robotics and Automation*, Seattle, WA, May 2015, pp. 4006–4013.

[10] M. Ryll, D. Bicego, and A. Franchi, "Modeling and control of FAST-Hex: a fully-actuated by synchronized-tilting hexarotor," in *2016 IEEE/RSJ Int. Conf. on Intelligent Robots and Systems*, Daejeon, South Korea, Oct. 2016.

[11] M. Mohammadi, A. Franchi, D. Barcelli, and D. Prattichizzo, "Cooperative aerial tele-manipulation with haptic feedback," in *2016 IEEE/RSJ Int. Conf. on Intelligent Robots and Systems*, Daejeon, South Korea, Oct. 2016.

[12] G. Gioioso, A. Franchi, G. Salvietti, S. Scheggi, and D. Prattichizzo, "The Flying Hand: a formation of uavs for cooperative aerial tele-manipulation," in *2014 IEEE Int. Conf. on Robotics and Automation*, Hong Kong, China, May. 2014, pp. 4335–4341.

[13] G. Gioioso, M. Mohammadi, A. Franchi, and D. Prattichizzo, "A force-based bilateral teleoperation framework for aerial robots in contact with the environment," in *2015 IEEE Int. Conf. on Robotics and Automation*, Seattle, WA, May 2015, pp. 318–324.

[14] B. Yüksel, N. Staub, and A. Franchi, "Aerial robots with rigid/elastic-joint arms: Single-joint controllability study and preliminary experiments," in *2016 IEEE/RSJ Int. Conf. on Intelligent Robots and Systems*, Daejeon, South Korea, Oct. 2016.

[15] B. Yüksel, G. Buondonno, and A. Franchi, "Differential flatness and control of protocentric aerial manipulators with mixed rigid- and elastic-joints," in *2016 IEEE/RSJ Int. Conf. on Intelligent Robots and Systems*, Daejeon, South Korea, Oct. 2016.

[16] B. Yüksel, S. Mahboubi, C. Secchi, H. H. Bülthoff, and A. Franchi, "Design, identification and experimental testing of a light-weight flexible-joint arm for aerial physical interaction," in *2015 IEEE Int. Conf. on Robotics and Automation*, Seattle, WA, May 2015, pp. 870–876.

[17] A. Censi, A. Franchi, L. Marchionni, and G. Oriolo, "Simultaneous maximum-likelihood calibration of odometry and sensor parameters," *IEEE Trans. on Robotics*, vol. 29, no. 2, pp. 475–492, 2013.